Journal of Thermal Analysis and Calorimetry, Vol. 83 (2006) 1, 125–130

DETECTION OF AUTOCATALYTIC DECOMPOSITION BEHAVIOR OF ENERGETIC MATERIALS USING APTAC

C. Wei, W. J. Rogers and M. S. Mannan[*]

Mary Kay O'Connor Process Safety Center, Department of Chemical Engineering, Texas A&M University, College Station
TX 77843-3574, USA

Characterization of autocatalytic decomposition reactions is important for the safe handling and storage of energetic materials. Isothermal differential scanning calorimetry (DSC) has been widely used to detect autocatalytic decomposition of energetic materials. However, isothermal DSC tests are time consuming and the choice of experimental temperature is crucial. This paper shows that an automatic pressure tracking calorimeter (APTAC) can be a reliable and efficient screening tool for the identification of autocatalytic decomposition behavior of energetic materials.

Hydroxylamine nitrate (HAN) is an important member of the hydroxylamine family. High concentrations of HAN are used as liquid propellants, and low concentrations of HAN are used primarily in the nuclear industry for decontamination of equipment. Because of its instability and autocatalytic decomposition behavior, HAN has been involved in several incidents.

This paper presents calorimetric measurements for the thermal decomposition of 24 mass% HAN/water. APTAC heat–wait–search and heat–soak–search modes are used to characterize the thermal decomposition of HAN. By comparing the kinetic analysis for the two modes, it is concluded that HAN shows strong autocatalytic decomposition behavior. The most likely decomposition pathway of HAN is proposed to explain the observed autocatalytic behavior.

Keywords: *APTAC, autocatalytic reactions, energetic materials, hydroxylamine nitrate*

Introduction

Hydroxylamine nitrate ($NH_2OH\cdot HNO_3$) is commercially available in clear and colorless water solutions, and it has been used primarily as a reductant in nuclear material processing and for decontamination of equipment. The U.S. Army has also explored the use of high concentrations of HAN as an oxidizer in a liquid propellant mixture. Due to its chemical properties, HAN has been involved in many incidents. On 14 May, 1997, an explosion occurred in the Chemical Preparation Room of the Plutonium Reclamation Facility at Hanford's Plutonium Finishing Plant. Thereafter, the U.S. Department of Energy investigated the incident and prepared a technical report on HAN/nitric acid mixture properties [1]. This report describes the autocatalytic decomposition behavior of HAN/nitric acid mixture and the effects of metal ions on the thermal decomposition in which the onset temperature of the autocatalytic reaction decreases with the increase of nitric acid to HAN ratio. In this paper, the autocatalytic decomposition of HAN without nitric acid is analyzed.

An autocatalytic reaction is a chemical reaction in which a product (or a reaction intermediate) acts as a catalyst [2], and the observed reaction rate is found to increase with time. This property poses a challenge for the prolonged storage of chemicals that can undergo autocatalytic decomposition. Chervin and Bodman [3] studied the autocatalytic decomposition phenomenon and kinetic models using isothermal DSC data. A screening method based on dynamic DSC measurement was developed to identify autocatalytic decomposition by Bou-Diab and Fierz [4]. According to this method, the decomposition is autocatalytic if the apparent activation energy calculated by a first order kinetic model is higher than 220 kJ mol^{-1}. Under adiabatic conditions, the temperature *vs.* time curves for n^{th} order reactions and autocatalytic reactions are different. For n^{th} order reactions, the temperature increase starts immediately after the onset temperature, while for autocatalytic reactions, the temperature increase is relatively small during the induction period and then suddenly grows rapidly. This paper presents the study of autocatalytic decomposition using APTAC heat–wait–search and heat–soak–search modes. The objective of this study is to explore the potential of adiabatic calorimeters to identify autocatalytic decomposition of energetic materials.

Experimental

Sample

Hydroxylamine nitrate (24 mass% in water solution, Aldrich catalog number 438235) was used without further purification and analysis.

---

[*] Author for correspondence: mannan@tamu.edu

1388–6150/$20.00

Akadémiai Kiadó, Budapest, Hungary
Springer, Dordrecht, The Netherlands

Automatic pressure tracking adiabatic calorimeter (APTAC)

Adiabatic calorimetry has proven to be an extremely useful tool to assess thermal hazards of reactive chemicals. It can minimize heat losses by maintaining the temperature of the sample surroundings as close as possible to the temperature of the sample. The APTAC calorimeter can be operated in a variety of test modes, such as heat–wait–search, heat ramps, and isothermal aging with temperatures up to 500°C and pressures ranging from vacuum to 13.8 MPa. It can track exotherms at heat generation rates from 0.04 to 400°C min^{-1}. It can produce low thermal inertia data, because it utilizes the DIERS pressure compensating technique in which the pressure outside the sample cell is controlled to match the pressure inside the sample cell. For the present work, HAN measurements were conducted in glass sample cells of nominal 100 cm^3, which can provide a neutral environment for the reactions, and also in titanium and stainless steel sample cells of nominal 130 and 50 cm^3, respectively, to test the effect of metals on the thermal decomposition. Teflon coated thermocouples were used to prevent the contact of hydroxylamine solution with thermal transmitter metals.

APTAC cannot directly measure heat of reaction, but the system of sample and sample cell was kept nearly adiabatic during runaway reaction. Therefore, part of the reaction heat was adsorbed by the sample cell, and the remainder was used to increase the temperature of the sample and vaporize volatile materials. The fact that sample heat capacity changes with temperature, composition, and phase changes makes it even more difficult to estimate the heat of the reaction from the experimental data. The liquid heat capacity of hydroxylamine nitrate is missing in the literature. Because water was the solvent and a major product in this experiment, the heat capacity of liquid water (4.18 J g^{-1} $°\text{C}^{-1}$) was used to estimate the thermal inertia ($\phi=(M_sC_s+M_bC_b)/M_sC_s$, where M is the mass, C is the heat capacity and subscripts b and s refer to the sample bomb and the sample, respectively). A detailed description of the APTAC can be found in the reference [5].

Methods

The APTAC heat–wait–search mode was used: the sample was heated at 2°C min^{-1} to a starting temperature, and the temperature was allowed to stabilize for 25 min, following which the APTAC searched for exothermic behavior. During the search period of 25 min, the temperature of the containment vessel gas was adjusted to match that of the sample. If the self-heat rate of the sample was greater than a preset threshold (0.05°C min^{-1}), the apparatus tracked the reaction adiabatically until the reaction ended or one of the shutdown criteria was met. If no exotherm was detected, the apparatus heated the sample to the next search temperature and the steps repeated until one of the shutdown criteria was met. The onset temperature is defined as the temperature when an exotherm is detected and it is usually the lowest temperature at which the sample self-heat rate surpasses the preset threshold (0.05°C min^{-1}) in the 'search' or 'adiabatic' mode.

The APTAC heat–soak–search mode was also used: the sample was heated to a certain soak temperature and held adiabatically. Every sixty minutes or if the sample temperature rose 1°C above the soak temperature, the self-heating rate would be polled and compared with a pre-defined sensitivity threshold. If the self-heating rate exceeded the threshold, a runaway reaction was detected and the sample was kept adiabatically. If the self-heating rate was less than the threshold, the sample would be cooled back to the soak temperature. The steps continued for a defined period. If it failed to detect self-heat at the end of soak period, the system would proceed with a standard heat–wait–search mode. The HSS method is generally used to test the effectiveness of inhibitors added to the reactants. In this study, the HSS method was employed to study the effect of autocatalysis on the decomposition of the reactive system. The autocatalysis would be generated during the soak period and thus allowed the reactants to eventually runaway in an adiabatic system when its concentration reached a certain level. Appropriate soak time and temperature should be chosen based on the knowledge of the reactive system.

A summary of APTAC test setup conditions is presented in Table 1. For the sample cell, the maximum allowable pressure imbalance is 1034 kPa. Due to the extremely rapid exothermic reactivity of hydroxylamine nitrate solution, it is difficult for the APTAC to track pressure rise fast enough, and the pressure imbalance was above 690 kPa even when small samples (about 4 g) were used in these tests. Stirring was not necessary because only small amounts of sample were used. To prevent undesired contaminations, the tubing lines between the sample cell and transducers and also the tubing leading to the on/off valve that closes the sample cell during tests were flushed with acetone following every experiment. The tubing was dried by flushing with compressed nitrogen.

Results and discussion

Heat–wait–search (HWS) result

The HWS mode was employed to determine the overall decomposition behavior of hydroxylamine nitrate, such as onset temperature (T_0), maximum temperature (T_{max}), maximum pressure (P_{max}), self-heating rate at

Table 1 Summary of the APTAC experimental setup conditions

Thermocouple	Teflon coated		
Heat mode	H–W–S/H–S–S		
Start temperature/°C	50/150	Minimum pressure/kPa	138
Limit temperature/°C	180	Over pressure/kPa	7
Temperature increment/°C	10	Lower band/kPa	–69
Cool down temperature/°C	50	Upper band/kPa	69
Exotherm threshold/°C	0.05	Exotherm limit/°C	300
Heat rate/°C min^{-1}	2	Soak time/min	1440
Stirring	NO		
Venting	NO		
Injection	NO		
Shut down criteria			
Temperature level/°C	300	Pressure level/kPa	8274
Heat rate/°C min^{-1}	400	Pressure rate/kPa min^{-1}	13790
Pressure imbalance/kPa	1034		

Table 2 APTAC HWS results of the thermal decomposition of hydroxylamine nitrate

HAN 4.2 g	T_0/ °C	T_{max}/ °C	P_{max}/ kPa	dT/dt_0/ °C min^{-1}	dT/dt_{max}/ °C min^{-1}	dP/dt_{max}/ kPa min^{-1}	Non-condensable/ kPa 50°C	Phi factor, ϕ	ΔH_{rxn}/ kJ mol^{-1}
Glass cell	171.3±0.2	196.1±0.7	2041±34	0.07±0.01	416±20	1200±386	283±7	3.3	–138±4
Ti cell	150.1±3.1	178.5±0.9	1338±21	0.06±0.01	279±50	193±48	179±14	2.0	–96±13
SS cell	139.2±3.2	168.9±1.7	1565±62	0.06±0	179±53	2027±372	379±7	3.6	–180±8

the onset temperature (dT/dt_0), maximum self-heating rate (dT/dt_{max}), heat of reaction (ΔH_{rxn}), and non-condensable product pressure at 50°C. The experimental results using glass, titanium, and stainless steel sample cells are presented in Table 2 and Figs 1 and 2. The effect of sample cell material on onset temperatures shows that a glass cell can provide a neutral environment, and metals such as titanium and stainless steel can catalyze the decomposition of hydroxylamine nitrate. Compared with glass, titanium initiates the decomposition at a lower temperature, but less heat is evolved from the reaction, while stainless steel can cause 30% more heat release from the decomposition.

The decomposition curve of hydroxylamine nitrate is compared with that of 50 mass% hydroxylamine/water in Fig. 3. Hydroxylamine nitrate decomposition starts at 170°C and the temperature increases slowly until 180°C at which point suddenly the temperature increases very rapidly to the maximum temperature of 196°C. The temperature curve of hydroxylamine nitrate appears to be two stages: a slow initiation stage followed by a fast explosion stage. These two stages form a sharp corner as emphasized by the circle in Fig. 3. On the contrary, for the decomposition of hydroxylamine, the temperature increase starts immediately after the onset temperature and smoothly curves up to the maximum temperature. Previous studies showed that hydroxylamine decomposition was a 1st order reaction with apparent activation energy of 121 kJ mol^{-1} [6]. From comparison of the decomposition temperature curves, it can be concluded that hydroxylamine nitrate decomposition is an autocatalytic reaction. Initially the decomposition shows only little heat release and therefore the temperature increase is slow. After an induction period, the concentration of the autocatalyst reaches a threshold level and the reaction rate becomes very rapid.

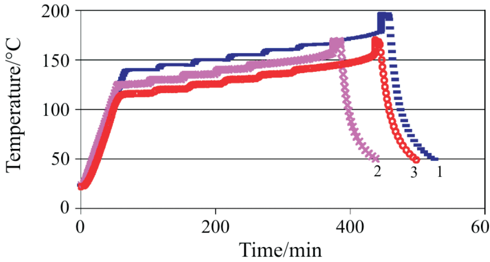

Fig. 1 Temperature *vs*. time profiles for HAN decomposition in 1 – glass, 2 – titanium and 3 – stainless steel sample cells

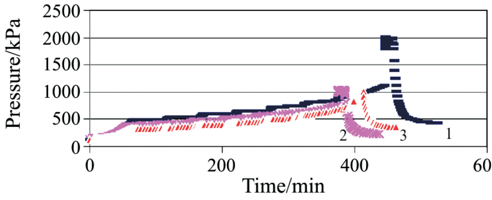

Fig. 2 Pressure *vs*. time profiles for HAN decomposition: in 1 – glass, 2 – titanium and 3 – stainless steel sample cells

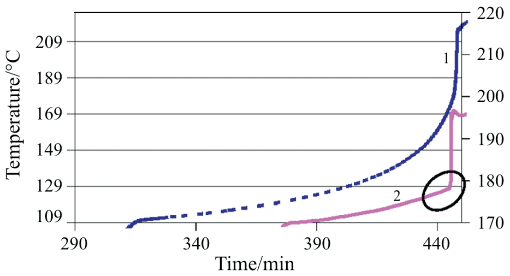

Fig. 3 Comparison of decomposition curve of hydroxylamine nitrate with hydroxylamine; 1 – HA, 2 – HAN

Heat–soak–search (HSS) result

In order to test the aging effect on the thermal decomposition of hydroxylamine nitrate, the HSS method was employed. The experimental results using glass, titanium, and stainless steel sample cells are presented in Table 3 and Figs 4–6. The soak temperatures were chosen as 20 degree lower than onset temperatures of the HWS results, and the soak period was 24 h. During the soak and search periods, although temperature is almost constant, the pressure increase is detected because the decomposition is undergoing with a low self-heat rate. In the titanium cell, a fast explosion occurred at the end of soak period of 24 h. In the glass and stainless steel cells, significant self-heat rates were not detected during the soak period, so the apparatus proceeded with the HWS mode. The detected onset temperatures are lower than the ones of the HWS mode alone. Besides the onset temperatures, the maximum self-heat rates and maximum pressure rates were also lower in Table 3 than the ones in Table 2. During the soak and search periods, the initiation reaction starts and autocatalyst is generated. If the self-heat rate is not sufficient, the temperature will be cooled down to the soak temperature. Therefore, some heat loss occurred during the soak period, and the estimated heats of reaction were reduced significantly in the HSS mode.

The self-heat rates of the HWS and HSS modes are compared in Fig. 7. The peaks correspond to the fast explosion, and the corresponding self-heat rate points seem like straight lines because the reaction is very fast. The temperature corresponding to the maximum self-heat rate is 15 degree lower in the HSS mode than that in the HWS mode. The fast explosion can occur at a significantly lower temperature because a significant amount of autocatalyst is accumulated during the soaking period of 24 h.

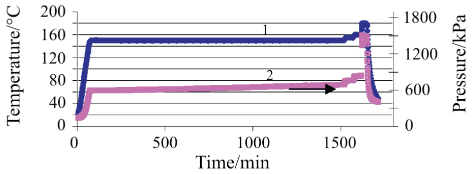

Fig. 4 HSS experimental results of hydroxylamine nitrate in a glass sample cell; 1 – temperature, 2 – pressure

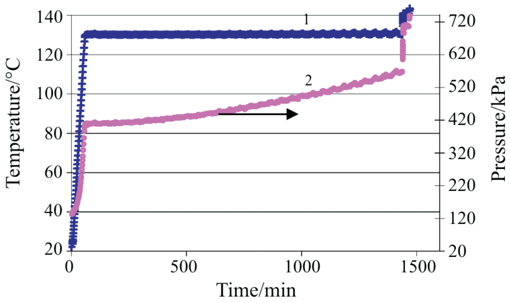

Fig. 5 HSS experimental results of hydroxylamine nitrate in a titanium sample cell; 1 – temperature, 2 – pressure

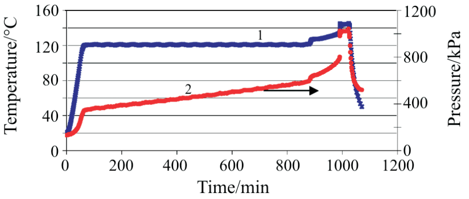

Fig. 6 HSS experimental results of hydroxylamine nitrate in a stainless steel sample cell; 1 – temperature, 2 – pressure

Kinetic analysis

In this study, assuming that the decomposition follows an n^{th} order reaction, the activation energies of the thermal decomposition of hydroxylamine nitrate were calculated from a pseudo zero-order rate constant, k^*, using the method developed by Townsend and Tou [7]. The Arrhenius parameters can be estimated from the straight lines fitting to lnk^* *vs.* $1000/T$ curves. The plots of lnk^* *vs.* $1000/T$ with a reaction order of 0.1 are given in Fig. 8. The self-heat rate of hydroxylamine nitrate decomposition increases very rapidly with temperature, therefore the straight lines in Fig. 8 have

Table 3 APTAC HSS results of the thermal decomposition of hydroxylamine nitrate

HAN 4.2g	Soak T/ °C	T_0/ °C	T_{max}/ °C	P_{max}/ kPa	dT/dt_0/ °C min^{-1}	dT/dt_{max}/ °C min^{-1}	dP/dt_{max}/ kPa min^{-1}	Non-condensable kPa (50°C)	Phi factor, ϕ	ΔH_{rxn}/ kJ mol^{-1}
Glass cell	150	165.4±5.3	183.9±4.7	1606±124	0.07±0.03	344±18	765±214	283±7	3.3	–172±7
Ti cell	150	131.2±1.1	143.2±4.7	710±83	0.05±0.02	128±51	83±28	165±7	2.0	–42±13
SS cell	120	127.3±2.1	140.2±4.8	945±76	0.07±0.02	139±39	41±14	365±7	3.6	–75±17

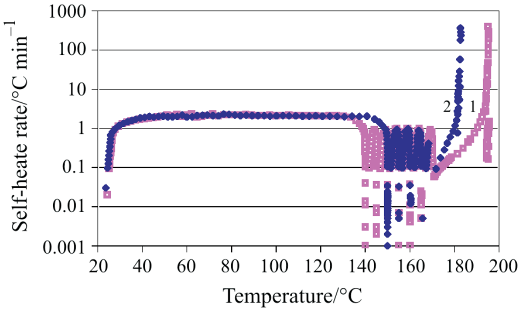

Fig. 7 Comparison of 1 – HWS and 2 – HSS experimental results of hydroxylamine nitrate in a glass cell

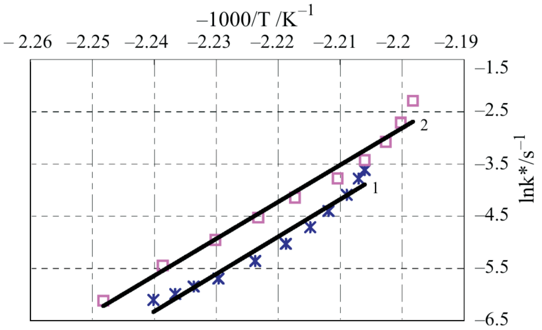

Fig. 8 Comparison of 1 – HWS and 2 – HSS kinetic analysis of hydroxylamine nitrate decomposition in a glass cell

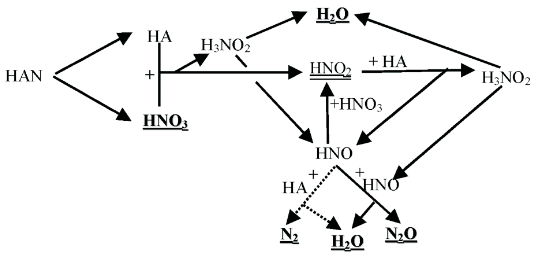

Fig. 9 Detailed mechanism of hydroxylamine nitrate decomposition. Species – final products; species – autocatalyst; HAN – hydroxylamine nitrate; HA – hydroxylamine; –– – dominant steps, --- – less dominant steps

steep slopes and correspondingly very high values of activation energies. The two straight lines obtained from the HWS and HSS experimental results are almost parallel, and corresponding activation energies are about the same value of 585 kJ mol^{-1}. At low temperatures, the rate constants of the HSS mode are higher than those of the HWS mode because autocatalyst has accumulated during the HSS mode.

Compared with other members of the hydroxylamine family [8], hydroxylamine nitrate has a large activation energy. Therefore, a very high activation energy obtained by fitting n^{th} order rate constant can be an information cue of autocatalytic behavior. However, in order to determine a boundary between an autocatalytic reaction and an n^{th} order reaction using activation energies, more experimental data sets are necessary.

Autocatalytic decomposition mechanism

Thermal decomposition products of hydroxylamine nitrate were analyzed to be nitric acid, water, and gas products (83% nitrous oxide, 17% nitrogen), and two overall Eqs (1), (2) of equal importance were proposed [9]. The decomposition pathway was also studied by a few groups [9, 10]. Based on information from the literature and quantum mechanical calculations using Gaussian 03 [11], a detailed decomposition mechanism is represented by a digraph in Fig. 9. Hydroxylamine nitrate is in equilibrium with nitric acid and hydroxylamine. The dissociated hydroxylamine reacts with nitric acid, producing nitrous acid, nitroxyl (HNO), and water most likely via an intermediate N-hydroxyl hydroxylamine (H_3NO_2). The intermediate nitrous acid is scavenged by hydroxylamine also via the intermediate H_3NO_2, producing nitroxyl and water. Nitroxyl can be either dimerized into nitrous oxide or scavenged by nitric acid to form nitrous acid, an important intermediate that causes the autocatalytic decomposition of hydroxylamine nitrate. A small amount of nitrogen is most likely due to interaction between nitroxyl and hydroxylamine.

$$3HONH_3^+\ NO_3^- \Rightarrow N_2O+N_2+2HNO_3+5H_2O \qquad (1)$$

$$4HONH_3^+\ NO_3^- \Rightarrow 3N_2O+2HNO_3+7H_2O \qquad (2)$$

Conclusions

The thermal decomposition of 24 mass% hydroxylamine nitrate/water was analyzed using the APTAC. From heat–wait–search and heat–soak–search modes experimental results, the decomposition shows strong autocatalytic behavior. Adiabatic calorimeter is also a promising technique to detect autocatalytic reaction. The temperature curve of autocatalytic reaction shows two stages: a slow initiation stage and a fast explosion stage. The explosion stage occurs very suddenly and quickly. By comparing HWS and HSS experimental results, the explosion stage can start at a much lower temperature after a certain aging period. From the kinetic analysis results, the apparent activation energy of an autocatalytic decomposition will be very large if an n^{th} order kinetic model is used to fit the adiabatic calorimetric data.

A plausible decomposition mechanism for hydroxylamine nitrate was proposed. Nitrous acid was found to be the intermediate that caused the autocatalytic behavior. In order to temper the autocatalytic reaction, the concentration of nitrous acid should be limited. Since nitrous acid was proposed to be generated from nitric acid, inadvertent addition of nitric acid to HAN may cause potential explosions. One way to control the concentration of nitrous acid was to use hydrazine (N_2H_2) [1], because it reacts faster with nitrous acid than HAN. However, hydrazine possesses hazardous properties and has potential for explosive formations. To handle HAN safely, low concentrations of HAN may be used, and contamination needs to must be avoided.

Acknowledgements

This research was supported by the Mary Kay O'Connor Process Safety Center at Texas A&M University. We would like to thank the Supercomputing Facility at Texas A&M University for computer time and the Laboratory for Molecular Simulation (LMS) at Texas A&M University for software and support. A discussion with Dr. Marc E. Levin from Shell Global Solutions was very helpful.

List of abbreviations

T_0	Onset temperature at which exothermic decomposition is first detected /°C
T_{max}	Max. temperature due to decomposition /°C
P_{max}	Max. pressure generated due to decomposition /kPa
dT/dt_0	Self-heating rate at onset temperature /°C min^{-1}
dT/dt_{max}	Max. self-heating rate /°C min^{-1}
ΔH_{rxn}	Heat of reaction /kJ mol^{-1}

Appendix

The likely reaction pathways are listed below. The enthalpy of each molecule was calculated using Gaussian 03 at the B3LYP/cc-PVDZ level of theory. The heats of reaction were calculated as $\Delta H_{rxn}=\Sigma\Delta H_{products}-\Sigma\Delta H_{reactants}$. The thermodynamically favored pathways are listed in bold.

Reaction schemes	ΔH_{rxn}/kJ mol^{-1}
$NH_2OH\cdot HNO_3\Leftrightarrow NH_2OH+HNO_3$	**74.0**
$NH_2OH+HNO_3\Rightarrow H_3NO_2+HNO_2$	**10.0**
$H_3NO_2\Rightarrow H_2O+HNO$	**–13.0**
$NH_2OH+HNO_3\Rightarrow N_2H_2O_3+H_2O$	43.9
$NH_2OH+HNO_3\Rightarrow HNO_2+HNO$	–46.8
$NH_2OH+HNO_3\Rightarrow NH_2O+H_2NO_3$	148.4
$NH_2O+H_2NO_3\Rightarrow HNO+HNO_2+H_2O$	–151.3
$HNO+HNO_3\Rightarrow HNO_2+HNO_2$	**–128.7**
$NH_2OH+HNO_3\Rightarrow NH_2O+NO_2+H_2O$	28.8
$NH_2O+NO_2\Rightarrow HNO_2+HNO$	–31.7
$HNO_2+NH_2OH\Rightarrow NH_2O_2+NH_2O$	142.1
$NH_2O_2+NH_2O\Rightarrow 2HNO+H_2O$	–16.3
$NH_2O_2\Rightarrow NO+H_2O$	–102.8
$NH_2O+NO\Rightarrow 2HNO$	86.5
$HNO_2+NH_2OH\Rightarrow H_3NO_2+HNO$	**138.7**
$2HNO\Rightarrow N_2O+H_2O$	**–351.9**
$HNO+NH_2OH\Rightarrow 2NH_2O$	**18.0**
$2NH_2O\Rightarrow N_2+2H_2O$	**–487.0**

References

1 Technical Report on Hydroxylamine Nitrate, in US Department of Energy, February 1998.
2 Compendium of Chemical Terminology, Ed. A. Wilkinson, Vol. 2nd Edition, 1997, Blackwell Scientific Publications: Oxford.
3 S. Chervin and G. T. Bodman, Thermochim. Acta, 392–393 (2002) 371.
4 L. Bou-Diab and H. Fierz, J. Hazard. Mater., 93 (2002) 137.
5 S. Chippett, P. Ralbovsky and R. Granville, The APTAC: a high pressure, low thermal inertia, adiabatic calorimeter, in International Symposium on Runaway Reactions, Pressure Relief Design, and Effluent Handling, 1998, New Orleans: American Institute of Chemical Engineers.
6 L. O. Cisneros, W. J. Rogers and M. S. Mannan, J. Hazard. Mater., 95 (2002) 13.
7 D. I. Townsend and J. C. Tou, Thermochim. Acta, 37 (1980) 1.
8 L. O. Cisneros, W. J. Rogers and M. S. Mannan, Thermochim. Acta, 414 (2004) 177.
9 J. C. Oxley and K. R. Brower, Proceedings of SPIE-The International Society for Optical Engineering, 872 (1988) 63.
10 J. W. Schoppelrei and T. B. Brill, J. Phys. Chem. A, 101 (1997) 8593.
11 Gaussian 03, Revision B.04, M. J. Frisch, G. W. Trucks, H. B. Schlegel, G. E. Scuseria, M. A. Robb, J. R. Cheeseman, J. A. Montgomery, Jr., T. Vreven, K. N. Kudin, J. C. Burant, J. M. Millam, S. S. Iyengar, J. Tomasi, V. Barone, B. Mennucci, M. Cossi, G. Scalmani, N. Rega, G. A. Petersson, H. Nakatsuji, M. Hada, M. Ehara, K. Toyota, R. Fukuda, J. Hasegawa, M. Ishida, T. Nakajima, Y. Honda, O. Kitao, H. Nakai, M. Klene, X. Li, J. E. Knox, H. P. Hratchian, J. B. Cross, C. Adamo, J. Jaramillo, R. Gomperts, R. E. Stratmann, O. Yazyev, A. J. Austin, R. Cammi, C. Pomelli, J. W. Ochterski, P. Y. Ayala, K. Morokuma, G. A. Voth, P. Salvador, J. J. Dannenberg, V. G. Zakrzewski, S. Dapprich, A. D. Daniels, M. C. Strain, O. Farkas, D. K. Malick, A. D. Rabuck, K. Raghavachari, J. B. Foresman, J. V. Ortiz, Q. Cui, A. G. Baboul, S. Clifford, J. Cioslowski, B. B. Stefanov, G. Liu, A. Liashenko, P. Piskorz, I. Komaromi, R. L. Martin, D. J. Fox, T. Keith, M. A. Al-Laham, C. Y. Peng, A. Nanayakkara, M. Challacombe, P. M. W. Gill, B. Johnson, W. Chen, M. W. Wong, C. Gonzalez and J. A. Pople, Gaussian, Inc., Pittsburgh PA, 2003.

DOI: 10.1007/s10973-005-6982-3